Available online at www.sciencedirect.com
SCIENCE DIRECT®
Journal of Catalysis 223 (2004) 296–308
JOURNAL OF CATALYSIS
www.elsevier.com/locate/jcat

Catalytic oxidation of chlorinated benzenes over V_2O_5/TiO_2 catalysts

Janine Lichtenberger and Michael D. Amiridis *

Department of Chemical Engineering. University of South Carolina, Columbia, SC 29208, USA

Received 9 October 2003; revised 27 January 2004; accepted 30 January 2004

Abstract

Kinetic and in situ infrared spectroscopic studies were conducted to investigate the oxidation of different chlorinated benzenes (i.e., chlorobenzene, 1,2- 1,3-, and 1,4-dichlorobenzene) over V_2O_5/TiO_2 catalysts. The oxidation of cyclohexyl chloride and that of benzene were also examined for comparison. Observed differences in the reaction rates and activation energies can be correlated to the structural differences of these compounds, in light of a common reaction mechanism. This mechanism is supported by the results of in situ FTIR studies, which indicate the presence of similar surface intermediates on the catalyst surface under reaction conditions for all the aromatic compounds examined. The results further suggest that the following two are the important mechanistic steps in the oxidation of chlorinated benzenes: (1) the adsorption of the aromatic compound on the catalyst via a nucleophilic attack on the chlorine position in the aromatic ring and (2) the subsequent oxidation of the remaining aromatic ring.

Keywords: Oxidation; Chlorinated aromatics; Air toxics; Vanadium oxide; FTIR

1. Introduction

In recent years, the incineration of municipal and medical waste has become the preferred method for waste treatment in large residential areas. In addition to the standard combustion by-products (i.e., CO, NO_x, SO_x), small amounts of toxic polychlorinated aromatic compounds (i.e., polychlorinated dibenzodioxins [PCDDs] and dibenzofurans [PCDFs]) are also present in the flue gas of waste incinerators. Stringent environmental regulations are in place in several countries limiting PCDD/PCDF emissions. In Germany, for example, the "17. BImSchVA vom 23.11.1990, BGB1 I, 2545" has placed a limiting value of 0.1 ng I-TEQ/($N\,m^3$) (i.e., International Toxicity Equivalents per $N\,m^3$) for PCDD/PCDF emissions from municipal and hazardous waste incinerators. Similar limits are also in effect in several other European countries since the early 1990s and in Japan since 1997 [1].

Currently, the catalytic oxidation of PCDD/PCDFs to carbon dioxide, HCl, and water is the best method for their destruction. V_2O_5/TiO_2-based catalysts, which are commercially employed for the reduction of NO_x via NH_3–SCR, have also been found to be active for the oxidation of PCDD/Fs [2,3]. The kinetics of the oxidation of chlorinated aromatic compounds over these systems have been studied by several groups [1,4–7]. Furthermore, Jones and Ross have investigated the combined removal of NO and chlorinated aromatics over supported vanadia catalysts [8] and showed that the two reactions proceed independently of each other. Model compounds have been used in the majority of these studies due to the high toxicity of PCDD/PCDFs. Chlorobenzenes, and in particular, 1,2-dichlorobenzene (*o*-DCB), have been most frequently used (e.g., [5,6,9–15]), because of their structural similarity to PCDDs.

Work focusing on the oxidation of *o*-DCB over supported vanadia catalysts has been carried out in our group by Krishnamoorthy and co-workers [10,16,17]. These studies demonstrated that V_2O_5 supported on either TiO_2 or Al_2O_3 is active for the oxidation of *o*-DCB. The turnover frequency of the reaction (i.e., the reaction rate per vanadium site) was found to be independent of the surface vanadia coverage, suggesting that only a single surface vanadia site is involved in the kinetically significant step(s). In situ FTIR spectroscopic studies of these catalysts under reaction conditions revealed that the benzene ring remains intact during the adsorption of the *o*-DCB molecule, and that several partially oxidized intermediates are formed. Nevertheless, the mechanistic aspects of the oxidation of chlorinated aromatics over V_2O_5/TiO_2-based catalysts are still not clearly understood. In our efforts to advance this understanding further, we have

* Corresponding author.
E-mail address: amiridis@engr.sc.edu (M.D. Amiridis).

0021-9517/$ – see front matter
doi:10.1016/j.jcat.2004.01.032

conducted kinetic and in situ FTIR spectroscopic studies of the oxidation of several different chlorinated organic compounds over V_2O_5/TiO_2 catalysts. In particular, we have examined the oxidation of different chlorinated benzenes (i.e., chlorobenzene, 1,2- 1,3-, and 1,4-dichlorobenzene), as well as the oxidation of cyclohexyl chloride and benzene. The kinetic and in situ FTIR results of these studies are presented in this paper and a common reaction mechanism is proposed for all cases.

2. Experimental

2.1. Catalyst preparation

The 3.6 wt% V_2O_5/TiO_2 catalyst used in this study was prepared by an impregnation procedure. Prior to the impregnation the TiO_2 support was calcined at 500 °C for 3 h. Ammonium metavanadate (NH_4VO_3) was utilized as the V_2O_5 precursor. An aqueous solution of ammonium metavanadate was prepared and heated slowly until all of the precursor was completely dissolved. This solution was then added to an aqueous TiO_2 slurry. The resulting solution was stirred and heated until all the water was evaporated. Samples thus obtained were dried overnight in a vacuum oven at 80 °C, and then slowly heated to 520 °C in 8 h and calcined in air at this temperature for 2 h. During the calcination the ammonium metavanadate precursor was decomposed to yield vanadium oxide. The final vanadia loading of the catalyst was obtained through ICP measurements (Galbraight), while its surface area (69 m^2/g) was obtained through a BET measurement.

2.2. Kinetic studies

Kinetic measurements were carried out in a quartz, single-pass, fixed-bed reactor. A K-type thermocouple was placed into the catalyst bed to monitor the reaction temperature. The concentrations of the organic reactant in the reactor inlet and exit streams were determined online with a gas chromatograph (SRI 8610) equipped with either a 1/8 inch packed silica gel or a 1% AT1000 on chromosorb WHP column and a flame ionization detector. Each run utilized approximately 250 mg of catalyst in the form of 80 to 120 mesh (125–177 μm) particles. The volumetric flow through the catalyst bed was held constant at 222 ml/min (measured at atmospheric pressure and room temperature) for all kinetic measurements (corresponding space velocity of 53,000 cc/(g h)). Prior to each experiment, catalysts were pretreated in oxygen for 2 h at 500 °C. Liquid organic reactants (i.e., *o*-DCB, *p*-DCB, *m*-DCB, chlorobenzene, cyclohexyl chloride) were introduced to the reactor system by passage of a He stream through a saturator maintained at the appropriate temperature. The saturated He stream was further mixed with He and oxygen so that the desired inlet concentrations of 500–700 ppmv organic and 10% O_2 were achieved. Benzene was introduced directly as a gas mixture from a cylinder containing 1100 ppmv C_6H_6 in He. The conversions of the different reactants were calculated by subtracting the outlet concentration from the inlet concentration of the reactant and dividing by the inlet concentration. These conversions were obtained at different temperatures once steady state was reached at each temperature (i.e., the outlet concentration was not changing by more than 2% over a 1 h period). A random sequence of temperatures was chosen in each case, with some temperatures repeated toward the end of the sequence to assure reproducibility and rule out catalyst deactivation.

Experiments carried out with catalyst particles of different sizes demonstrated the absence of any internal diffusional limitations in our system in the 200–400 °C temperature range provided that the conversion of the organic reactant remained below 30%. Furthermore, in a previous study [10] we reported that carbon balances could be closed within 5% and only CO and CO_2 were detected in the analysis of the products. In particular, during the oxidation of *o*-DCB, in which case a detailed product analysis was performed the selectivity toward CO was in the range of 40–45%.

2.3. In situ FTIR studies

FTIR spectra were collected with a Nicolet 740 spectrometer and a homemade in situ flow cell. The spectrometer was equipped with a MCT-B detector cooled by liquid nitrogen. The cell had a path length of 10 cm and both ends were "capped" by IR-transparent NaCl crystal windows. Approximately 18–20 mg of the catalyst sample was pressed into a self-supported disk of approximately 1 cm in diameter. This disk was placed in a sample holder located at the center of the cell. The cell was wrapped with heating tape, and the temperature was measured with a thermocouple, placed close to the catalyst sample. Transmission spectra were collected in a single beam mode with a resolution of 2 cm^{-1}.

Prior to each experiment the catalyst was oxidized at 350 °C for 2 h. After the oxidation treatment the cell was flushed with He for at least 15 min and cooled down to the desired temperature in flowing He. The temperatures were chosen to correspond to a conversion of approximately 15–20% observed in the kinetic experiments. Spectra of the clean catalyst surface were collected after this process and utilized as the background. Subsequently, a mixture of He and the organic reactant (i.e., *m*-DCB, benzene, or cyclohexyl chloride) was introduced into the cell, at a concentration of approximately 500 ppmv. In situ FTIR spectra were collected next at different time intervals until a steady state was reached. Finally, the cell was flushed with He and/or a 10% O_2/He mixture to examine the strength of adsorption and the reactivity of the different surface species formed.

In situ FTIR experiments were also conducted with both the organic compound and the O_2 flowing together over the catalyst sample. The concentrations used for these studies were approximately 500 ppmv of the organic reactant and 10% O_2 in He. In this case, the reference spectra used as the

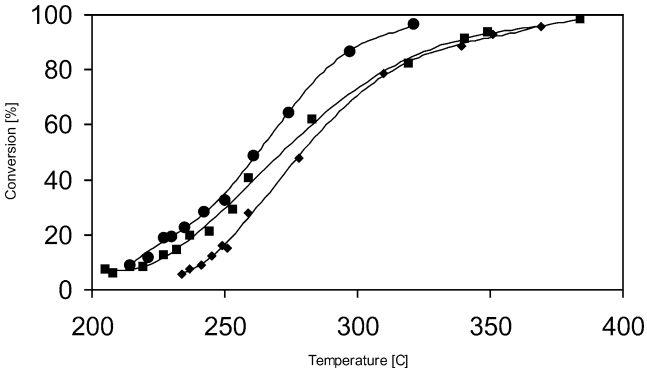

Fig. 1. Effect of temperature on the oxidation of benzene, chlorobenzene, and *m*-dichlorobenzene over a 3.6 wt% V_2O_5/TiO_2 catalyst; (■) *m*-DCB, (●) chlorobenzene, (◆) benzene (500 ppmv chlorobenzene and benzene, 700 ppmv *m*-DCB, 10% O_2, space velocity of 53,000 cc/(g h)).

background were collected at the reaction temperature in a flowing 10% O_2/He mixture.

In addition to the organic compounds noted above, the adsorption of phenol, maleic anhydride, and catechol on V_2O_5/TiO_2 was also studied by FTIR in order to confirm certain peak assignments.

3. Results and discussion

3.1. Kinetic results

The conversions of chlorobenzene, benzene, and 1,3-dichlorobenzene (*m*-DCB) over the 3.6 wt% V_2O_5/TiO_2 catalyst studied are shown as functions of temperature in Fig. 1. The results indicate that the rate of oxidation for this set decreases in the following order:

chlorobenzene > *m*-DCB > benzene.

Furthermore, the shapes of the light-off curves for these three aromatics in the low conversion regime (i.e., below 30%) appear to be different. Indeed, when an Arrhenius plot is obtained (Fig. 2), a significant difference in the activation energies is revealed (Table 1). In particular, *m*-DCB exhibits the lowest activation energy, followed by chlorobenzene and benzene, indicating that the ease of activation of these molecules increases with the degree of chlorination.

Table 1
Activation energies for the oxidation of different organic compounds over V_2O_5/TiO_2

Organic compound	Activation energy (kJ/mol)
Benzene	145 (±3)
Chlorobenzene	96 (±2)
ortho-DCB	82 (±4)
meta-DCB	80 (±2)
para-DCB	75 (±2)
Cyclohexyl chloride	32 (±3)

The experimental errors were calculated using linear regression.

The effect of the degree of chlorination of chlorobenzenes on the rate of their oxidation has been previously investigated by Furrer et al. [18]. This group examined the oxidation of chlorobenzene, 1,2-dichlorobenzene, and 1,2,4-trichlorobenzene over a $V_2O_5/WO_3/TiO_2$ catalyst and reported that the observed conversions of these chlorobenzenes were the same regardless of the degree of chlorination. However, the resolution of the activity measurements in that study may have not been sufficient to discern the effects observed in our work. In contrast, Weber et al. [1] reported that the rate of oxidation of chlorobenzenes (i.e., 1,2-dichlorobenzene, 1,2,3-trichlorobenzene, 1,2,4,5-tetrachlorobenzene, hexachlorobenzene) decreases with increasing degree of chlorination due to an "increasing redox potential." The same trend was observed in the present study with monochlorobenzene and dichlorobenzene. The same authors also investigated the effect of chlorine substitution on the rate of oxidation of dibenzofurans and dibenzodioxins and reported that in these cases the rate of oxidation is lowered with increasing degree of chlorination due to the electron-withdrawing effect of chlorine toward the aromatic ring system.

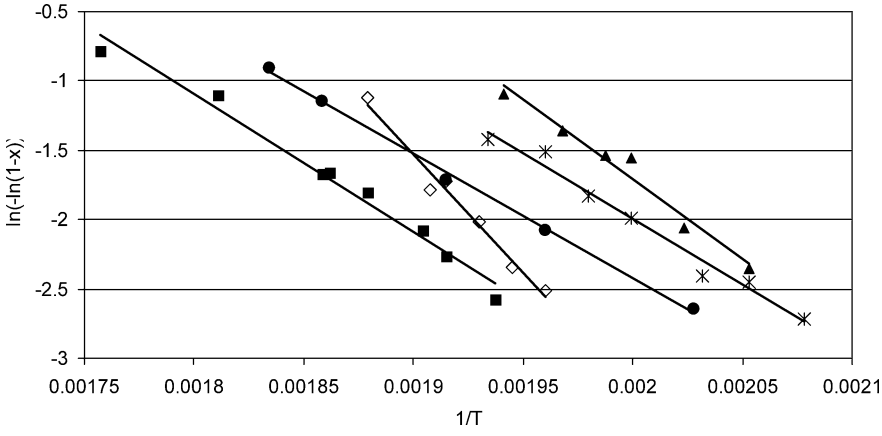

Fig. 2. Arrhenius plot for the oxidation of benzene, chlorobenzene, and the three dichlorobenzene isomers over a 3.6 wt% V_2O_5/TiO_2 catalyst; (◇) benzene, (▲) chlorobenzene, (∗) *m*-DCB, (●) *p*-DCB, (■) *o*-DCB (500 ppmv monochlorobenzene and benzene, 700 ppmv *o*-DCB, *m*-DCB, and *p*-DCB, 10% O_2, space velocity of 53,000 cc/(g h)).

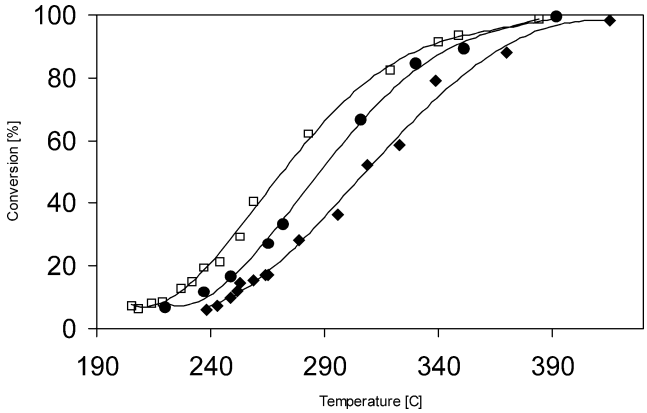

Fig. 3. Effect of temperature on the oxidation of *o*-DCB, *m*-DCB, and *p*-DCB over a 3.6 wt% V_2O_5/TiO_2 catalyst; (□) *m*-DCB, (◆) *o*-DCB, (●) *p*-DCB (700 ppmv *o*-DCB, *m*-DCB, and *p*-DCB, 10% O_2, space velocity of 53,000 cc/(g h)).

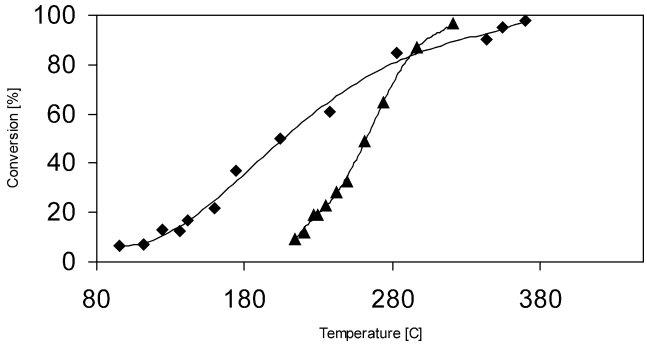

Fig. 4. Effect of temperature on the oxidation of chlorobenzene and cyclohexyl chloride over a 3.6 wt% V_2O_5/TiO_2 catalyst; (◆) cyclohexyl chloride, (▲) chlorobenzene (500 ppmv cyclohexyl chloride and chlorobenzene, 10% O_2, space velocity of 53 000 cc/(g h).

The conversions of *o*-DCB, *m*-DCB, and *p*-DCB over the 3.6 wt% V_2O_5/TiO_2 catalyst studied are shown as functions of temperature in Fig. 3. According to these results the rate of oxidation of the three different dichlorobenzenes decreases in the following order,

m-DCB > *p*-DCB > *o*-DCB,

suggesting that the relative position of the Cl atom affects the rate of oxidation of the different dichlorobenzenes. These differences indicate that the rate of oxidation depends on the charge distribution of the three molecules. The activation energies for the oxidation of the three dichlorobenzene isomers are approximately the same as shown in Table 1.

Finally, the conversions of chlorobenzene and cyclohexyl chloride over the 3.6 wt% V_2O_5/TiO_2 catalyst studied are shown as functions of temperature in Fig. 4. A much higher activity toward the oxidation of cyclohexyl chloride was observed in this case. Furthermore, a significantly lower activation energy was obtained with the nonaromatic molecule. These results suggest that the destruction of the aromatic ring is a kinetically significant step during the oxidation process.

3.2. *In situ FTIR studies*

3.2.1. *m-DCB and benzene*

3.2.1.1. TiO_2 FTIR spectra collected at different time intervals during the adsorption of *m*-DCB onto the pure titania support at 250 °C and the subsequent exposure of the catalyst to an O_2/He mixture are shown in Fig. 5.

The spectra of Fig. 5 include several bands that can be assigned to a surface phenolate species. In particular bands at 1575 and 1468 and a shoulder at 1442 cm^{-1} can be assigned to the C=C stretching vibrations, bands at 1252,

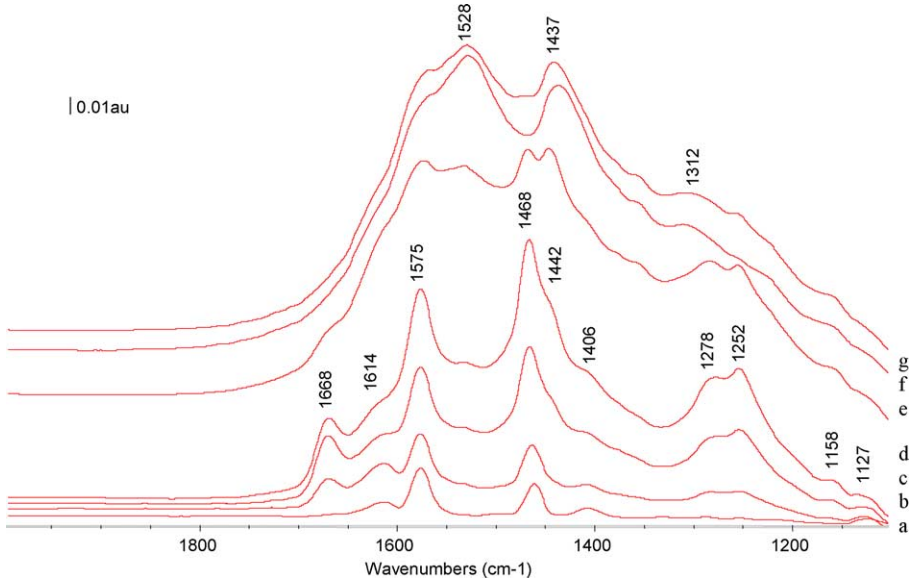

Fig. 5. In situ FTIR spectra of TiO_2 collected at 250 °C after (a) 1, (b) 20, (c) 40, and (d) 60 min on a 500 ppm *m*-DCB/balance He stream followed by (e) 1 min, (f) 20 min, and (g) 60 min exposure of the adsorbed species to a 10% O_2/He mixture.

Table 2
FTIR assignments of the adsorbed surface species

Organic reagent	Conditions	Catalyst	Wavenumber (cm^{-1})	Assignment	Supporting references
m-DCB	Adsorption	TiO_2	1575, 1468, 1442	Phenolate (C=C stretching)	[19–22]
			1252, 1158, 1127	Phenolate (CH in plane bending)	[19–22]
			1278	Phenolate (C–O stretching)	[19–22]
			1668, 1406	*o*-Benzoquinone	[19]
			1614	Vibration of aromatic ring adsorbed parallel to the surface	[19,23]
m-DCB	Oxidation	TiO_2	1528, 1437, 1312	Maleate	[19,26,27]
m-DCB	Adsorption	V_2O_5/TiO_2	1608	Vibration of aromatic ring adsorbed parallel to the surface	[19,23]
			1575, 1468	Phenolate (C=C stretching)	[19–22]
			1251	Phenolate (CH in plane bending)	[19–22]
			1220	Phenolate (C–O stretching on V_2O_5)	[19,20]
			1515, 1436, 1312, 1167	Maleate	[19,26,27]
			1551	Acetate (asymmetric stretching vibration)	[17,29–31]
			1444	Acetate (symmetric stretching vibration)	[17,29–31]
			1352	Acetate (CH_3 stretching vibration)	[32]
m-DCB	Oxidation	V_2O_5/TiO_2	1616, 1563, 1410, 1254	Chlorinated acetate/acetyl halide	[30,33,34]
			1755	Aldehyde-type species (C=O)	[30,36]
Benzene	Adsorption	TiO_2	1614	Vibration of aromatic ring adsorbed parallel to the surface	[19,23]
Benzene	Adsorption	V_2O_5/TiO_2	1608	Vibration of aromatic ring adsorbed parallel to the surface	[19,23]
			1575, 1468	Phenolate (C=C stretching)	[19–22]
			1515, 1436, 1312, 1167	Maleate	[19,26,27]
			1561	Acetate (asymmetric stretching vibration)	[17,29–31]
			1352	Acetate (CH_3 stretching vibration)	[32]
			1688, 1410, 1323	*o*-Benzoquinone	[35]

1158, and 1127 cm^{-1} to the C–H in-plane bending vibrations, and a band at 1278 cm^{-1} to the C–O stretching vibration of an adsorbed phenolate species (Table 2). Similar bands were observed during the adsorption of phenol on a 10 wt% V_2O_5/TiO_2 catalyst [19], on V/Ti and V/Zr catalysts [20], and on the TiO_2 support [21], as well as during the adsorption of chlorophenol on iron oxide [22]. Hence, the adsorption of *m*-DCB on TiO_2 proceeds through the formation of a surface phenolate.

Furthermore, a band at 1668 together with a shoulder at 1406 cm^{-1} observed in the spectra of Fig. 5 can be assigned to a surface *o*-benzoquinone-type species [19] (Table 2). Both bands decrease rapidly in intensity during exposure to the O_2/He mixture (Fig. 5), in agreement with a previous report by Busca et al. [19] who concluded that this species is very labile upon heating in oxygen. It should be pointed out that a chlorinated benzoquinone is probably formed in our case.

Finally, the spectra of Fig. 5 also contain a weak band at approximately 1614 cm^{-1}. This band is present after only 1 min on stream, but does not grow with time on stream as do the bands corresponding to the surface phenolate and benzoquinone species. Following adsorption of benzene onto the titania support at the same temperature, only a single band at 1614 cm^{-1} was observed (Fig. 6). Even at elevated temperatures of up to 300 °C the adsorption of benzene on TiO_2 does not yield any surface phenolate species (in contrast to that of *m*-DCB), indicating that vanadia is required for the activation of the unsubstituted benzene ring. This observation is consistent with the activation energies observed during the kinetic experiments. Finally, when the flow of benzene is stopped and the titania surface is exposed to gas-phase oxygen the band at 1614 cm^{-1} disappears quickly (Fig. 6). However, no evidence for the formation of any oxidation products can be found in this case, suggesting that the 1614 cm^{-1} band belongs to a labile adsorbed species that is not oxidized on TiO_2.

Busca et al. [19] also observed a strong band at 1611 cm^{-1} during the adsorption of benzene and *p*-benzoquinone on vanadia–titania catalysts and assigned it to the ring vibration of a substituted surface aromatic compound. Furthermore, van Hengstum et al. [23] detected a band at approximately 1600 cm^{-1} during the adsorption of toluene, xylene, benzaldehyde, and tolualdehyde on V_2O_5/TiO_2 and assigned it to the ring vibration of the resulting surface species. Finally, Street et al. [24] conducted adsorption studies of benzene on MgO using temperature-programmed desorption and high-resolution electron energy loss spectroscopy and concluded that benzene chemisorbs nondissociatively in this case. The ring plane is essentially parallel to the catalyst surface at low

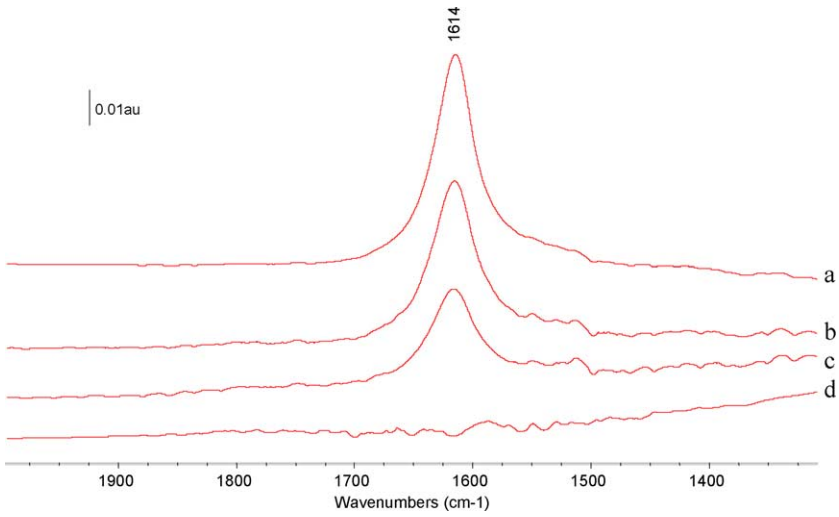

Fig. 6. In situ FTIR spectra of TiO_2 collected after 10 min at (a) 250 °C, (b) 280 °C, and (c) 300 °C on a 500 ppm benzene/balance He stream. Spectrum (d) was collected following 10 min exposure of (c) to a 10% O_2/He mixture.

surface coverages, but becomes perpendicular to the surface at elevated coverages. Hatayama et al. [25] also reported that the adsorption of benzene on V_2O_5/TiO_2 and ZrO_2/V_2O_5 occurs with the aromatic ring being parallel to the catalyst surface, while the adsorption of phenol proceeds with the ring being perpendicular to the surface. Based on the above we assign the band at 1614 cm^{-1} to a ring vibration of an aromatic compound adsorbed planar to the surface (Table 2). We can further speculate that perpendicular adsorption is required for the oxidation to proceed. While this can be easily accomplished even on the bare TiO_2 support with *m*-DCB, it does not take place with benzene in the absence of V_2O_5.

All species observed during the adsorption of the *m*-DCB onto the titania support are ring structures, suggesting that the molecule adsorbs without bond breaking of the aromatic ring. Hence, we conclude that the bond breaking of the aromatic ring requires the presence of gas-phase oxygen or vanadia (see next section). Indeed, the intensity of the bands corresponding to surface phenolates decreases slowly during exposure to a 10% O_2/He mixture (Fig. 5) At the same time new bands are observed at 1528, 1437, and 1312 cm^{-1} which can be assigned to a surface maleate species [19,26, 27] (Table 2). These results indicate that the oxidation and bond breaking of the activated aromatic ring takes place under these conditions.

3.2.1.2. V_2O_5/TiO_2 Spectra collected during the adsorption of *m*-DCB and benzene on the 3.6 wt% V_2O_5/TiO_2 catalyst studied are shown in Figs. 7 and 8, respectively. These spectra were collected at 250 and 260 °C for *m*-DCB and benzene, respectively. At these temperatures the observed conversions during the kinetic studies described in the previous sections were approximately 25% for *m*-DCB and 27% for benzene. Spectra collected at the same temperatures following the removal of the organic species from the gas phase, and flushing of the cell with either He or a 10% O_2/He mixture, are shown in Figs. 9 and 10.

Bands corresponding to surface phenolates (1575 and 1468 cm^{-1}), as well as some weaker not well-defined features between 1200 and 1300 cm^{-1} are observed in the spectra of both *m*-DCB and benzene (Figs. 7 and 8) and are more prominent during the first few minutes of adsorption. An additional weak band at approximately 1220 cm^{-1} can also be attributed to the C–O stretching frequency of a surface phenolate on V_2O_5. Busca et al. [19] observed a similar band (at 1210–1225 cm^{-1}) during the adsorption of phenol on a monolayer V_2O_5/TiO_2 catalyst, while Miyata et al. [20] observed the C–O stretching of phenolates at 1280 cm^{-1} on TiO_2 and 1210 cm^{-1} on V_2O_5.

While only phenolate bands were observed during the adsorption of *m*-DCB on the TiO_2 support (Fig. 5), additional bands are also present in the presence of vanadia (Fig. 7), indicating further oxidation of the phenolates and the formation of partial oxidation products. This is not a surprising result since vanadia can donate oxygen undergoing a reduction step. Furthermore, in the case of benzene the presence of vanadia is required even for the initial formation of the phenolates. The formation of additional partial oxidation products in the absence of gas-phase oxygen indicates that this reaction involves surface oxygen. The intensities of the bands corresponding to the surface phenolates decrease significantly upon removal of *m*-DCB and benzene from the gas-phase (Figs. 9 and 10), indicating that the oxidation of these species by surface oxygen is a relatively fast step. Finally, it should be noted that the concentration of surface phenolates is slightly higher following adsorption of *m*-DCB as compared to benzene, indicating that their formation is faster in this case, which is consistent with our observations during adsorption on the TiO_2 support.

The most pronounced partial oxidation products observed in Figs. 7 and 8 are surface maleates. The two main bands corresponding to maleates shift to slightly lower wavenumbers on the V_2O_5/TiO_2 catalyst (i.e., 1515 and 1436 cm^{-1}) as compared to the TiO_2 support. A new band observed at

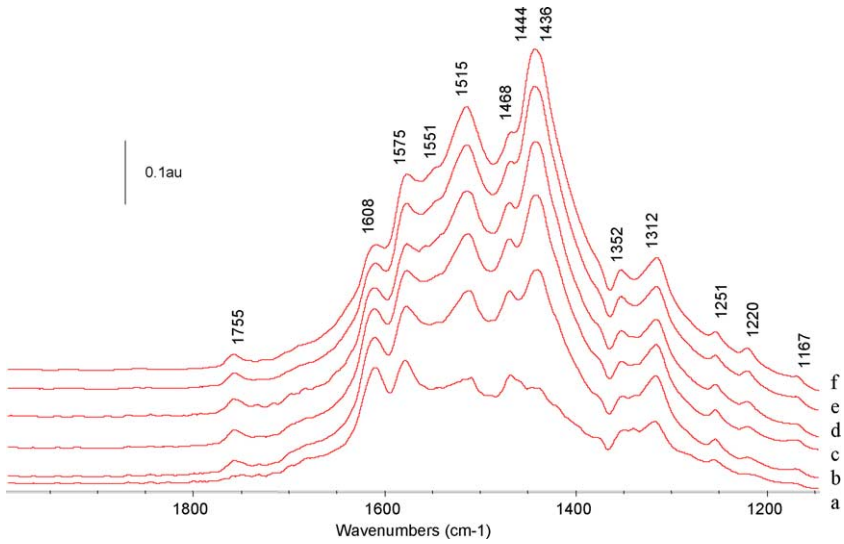

Fig. 7. In situ FTIR spectra of a 3.6 wt% V_2O_5/TiO_2 catalyst collected at 250 °C after (a) 3, (b) 10, (c) 20, (d) 40, (e) 80, and (f) 120 min on a 500 ppm *m*-DCB/balance He stream.

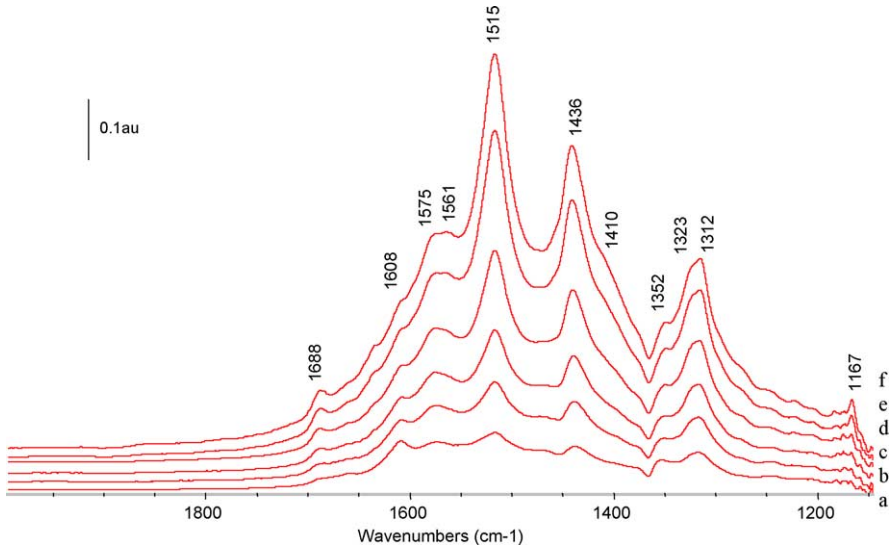

Fig. 8. In situ FTIR spectra of a 3.6 wt% V_2O_5/TiO_2 catalyst collected at 250 °C after (a) 3, (b) 10, (c) 20, (d) 40, (e) 80, and (f) 120 min on a 500 ppm benzene/balance He stream.

1167 cm^{-1} can also be assigned to a maleate species, since it was also observed during the adsorption of maleic anhydride on the V_2O_5/TiO_2 catalyst. A similar band at 1162 cm^{-1} has been previously assigned by Lin-Vien et al. [28] to the C–O stretching vibration of maleic anhydride in the gas phase. The 1167 cm^{-1} band was not observed on the pure titania, probably due to an overlap with stronger phenolate bands. The surface maleate species observed are fairly stable during exposure to helium and/or a 10% oxygen/helium mixture (Figs. 9 and 10), indicating that their further oxidation is very slow and they may represent spectator species on the catalyst surface.

During adsorption of *m*-DCB on the V_2O_5/TiO_2 a strong band was also observed at 1444 cm^{-1} (partially overlapped by the maleate band in this region) along with a shoulder at 1551 cm^{-1} (Fig. 7). These bands can be assigned to the COO^- stretching vibration of surface acetates [17,29–31]. In particular, the band at 1551 cm^{-1} is attributed to the COO^- asymmetric stretching vibration, while the band at 1444 cm^{-1} is attributed to the COO^- symmetric stretching vibration of these surface acetate species (Table 2). An additional band at 1352 cm^{-1} can also be assigned to the CH_3 stretching vibration of an acetate [32]. Bands at 1561 and 1352 cm^{-1} are also present during the adsorption of benzene on the V_2O_5/TiO_2 (Fig. 8). However, the band at 1444 cm^{-1} is not detectable, probably because of an overlap by the stronger maleate band in the same region. Once again, the surface acetate species are present on the catalyst surface in both the presence and the absence of gas-phase oxygen, indicating that surface oxygen is involved in their formation. The

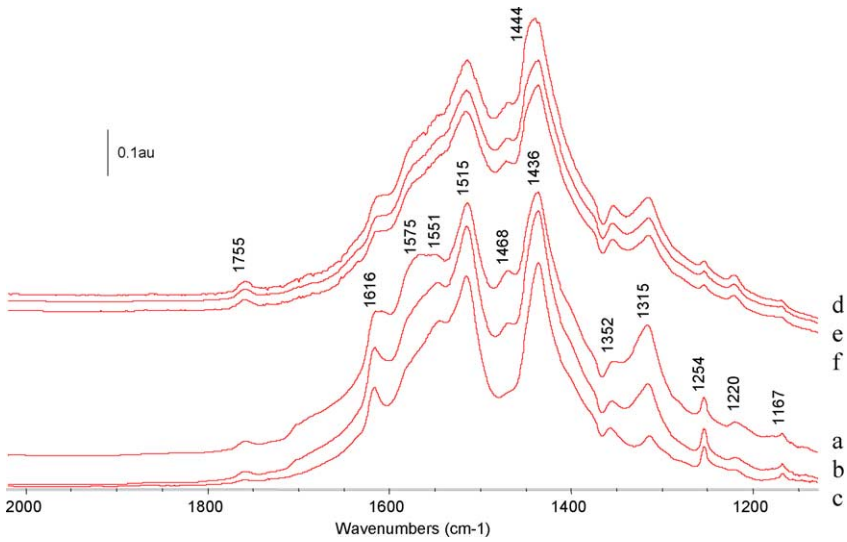

Fig. 9. In situ FTIR spectra of a 3.6 wt% V_2O_5/TiO_2 catalyst collected at 250 °C after adsorption of *m*-DCB and after (a) 1, (b) 10, and (c) 60 min exposure of the adsorbed species to a 10% O_2/He and after (d) 10, (e) 40, and (f) 60 min exposure of the adsorbed species to He.

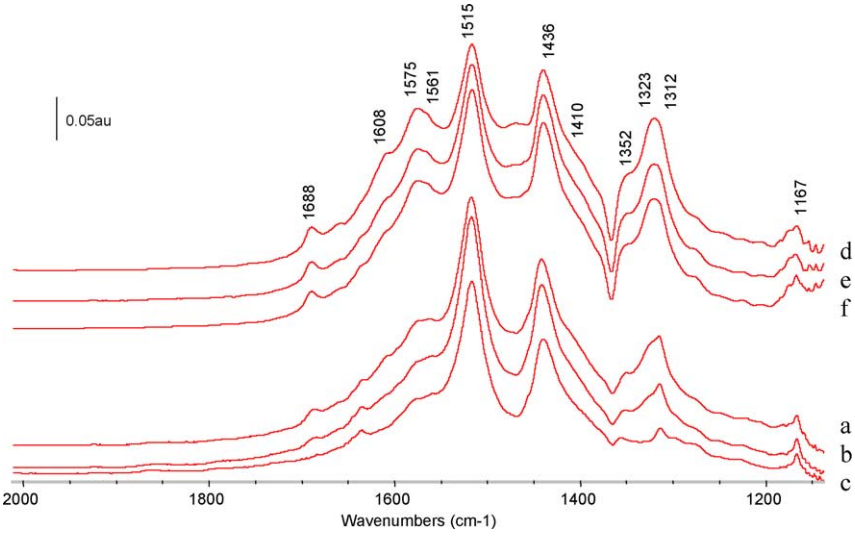

Fig. 10. In situ FTIR spectra of a 3.6 wt% V_2O_5/TiO_2 catalyst collected at 250 °C after adsorption of benzene and after (a) 1, (b) 10, and (c) 60 min exposure of the adsorbed species to a 10% O_2/He and after (d) 10, (e) 40, and (f) 60 min exposure of the adsorbed species to He.

intensity of the acetate bands decreases slowly upon desorption in He (Figs. 9 and 10), indicating their relatively high stability on the catalyst surface. However, they react faster in the presence of gas-phase oxygen (Figs. 9 and 10). The maleate bands are more pronounced than the acetate bands during the adsorption/ reaction of benzene. The opposite is observed during the adsorption/ reaction of *m*-DCB.

Upon exposure of the V_2O_5/TiO_2 catalyst to a 10% He/O_2 mixture following the adsorption of *m*-DCB, bands at 1616 and 1254 cm^{-1} grow in intensity (Fig. 9). The same bands are observed when the catalyst is exposed to the complete reaction mixture (Fig. 11), indicating that gas-phase oxygen enhances the formation of the corresponding surface species. These bands are not present in the spectra of adsorbed benzene, suggesting a possible assignment to a chlorinated species. Spectra collected during the oxidation of *m*-DCB (Fig. 11) also include a weak band at 1563 cm^{-1} and a shoulder at approximately 1410 cm^{-1}. Both bands belong to the same species, since upon removal of *m*-DCB from the gas phase they decrease in intensity simultaneously. Spinner [33] reported the presence of bands at 1603 and 1418 cm^{-1} (COO^- stretching vibrations) and 1250 cm^{-1} (CH_2 twist) in the IR spectra of solid $CH_2ClCOONa$. Furthermore, Chintwar and Greene [30] reported that the symmetric and asymmetric COO^- stretching vibrations of surface chlorinated acetate species formed on a Cr–Y zeolite shift either toward higher (for the asymmetric) or lower (for the symmetric) frequencies from the observed values for the corresponding nonchlorinated acetates, and assigned bands at 1591 and 1408 cm^{-1} to a chlorinated surface acetate species derived from perchloroethylene. Ng et al. [34] also reported similar shifts for fluorinated acetates adsorbed on alumina. Based on

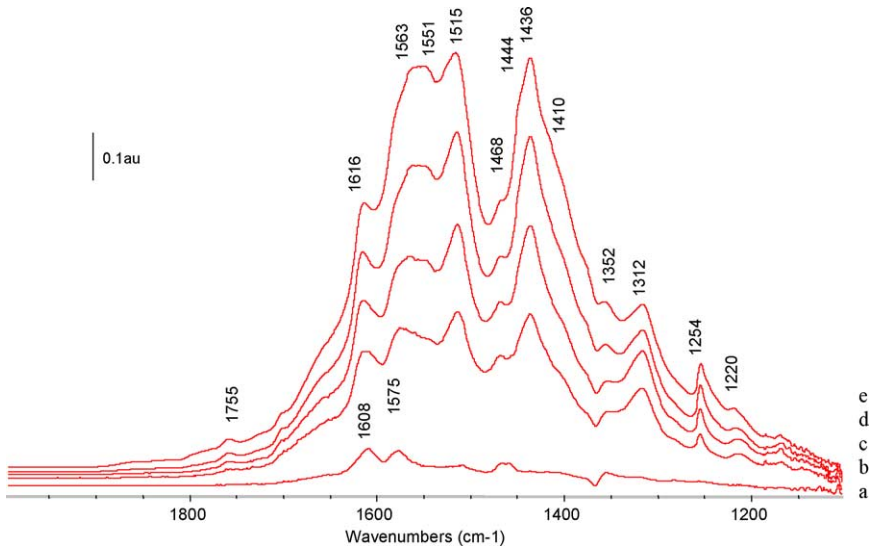

Fig. 11. In situ FTIR spectra of a 3.6 wt% V_2O_5/TiO_2 catalyst collected at 250 °C after (a) 1, (b) 5, (c) 10, (d) 20, and (e) 60 min on a 500 ppm *m*-DCB/10% O_2/balance He stream.

these reports we assign the observed bands at 1616, 1254, 1563, and 1410 cm^{-1} to chlorinated surface acetates and/or acetyl halides, such as CH_3COCl^- or CH_2ClCOO^- (Table 2).

During the adsorption of benzene (Fig. 8) a low intensity band was observed at 1688 cm^{-1}, the typical region of the C=O stretching frequency of quinones. Additional weak bands at 1323 and 1410 cm^{-1} were also observed to grow together in intensity with the band at 1688 cm^{-1} during adsorption (Fig. 8). These bands are stable during the exposure of the catalyst to He, but decrease in the presence of an O_2/He mixture (Fig. 10). Similar bands were observed by Otting and Staiger [35] for *o*-benzoquinone in KBr. A shift is evident in the position of these bands as compared to the ones assigned to an *o*-benzoquinone species formed during the adsorption of *m*-DCB onto the pure titania support. This shift may be due either to the degree of chlorination of the surface quinone species formed or to adsorption on titania versus vanadia. In both cases, the quinone species formed is not very stable upon desorption/reaction in O_2/He. It should be further noted that this surface quinone species was not detected during the adsorption/reaction of *m*-DCB on the V_2O_5/TiO_2 catalyst, suggesting that while the ring structure of benzene remains mostly intact after an electrophilic substitution during the second step in the proposed reaction mechanism (see Section 3.2.2), this is not the case with the substituted ring of *m*-DCB.

Finally, a low intensity band was detected at 1755 cm^{-1} during the adsorption/reaction of *m*-DCB (Figs. 7 and 11) on V_2O_5/TiO_2. Bands in this region are typical of the C=O stretching vibration of species containing a carbonyl group [30,36] and can be assigned to an aldehyde-type intermediate.

In summary, it appears that the same surface partial oxidation products (i.e., phenolates, quinones, maleates, and acetates) are formed during the adsorption and oxidation of benzene and *m*-DCB on the V_2O_5/TiO_2 catalyst studied, indicating that a similar oxidation pathway operates in both cases. However, differences in the relative intensities of the various IR bands, as well as differences observed in the kinetic results discussed in the previous section, suggest that the steps of this pathway proceed at different rates for the chlorinated and nonchlorinated compounds. The mechanistic implications of the IR results will be discussed in a subsequent section.

3.2.2. Cylohexyl chloride

FTIR spectra collected during the adsorption of cyclohexyl chloride on the V_2O_5/TiO_2 catalyst studied at 170 °C are shown in Fig. 12. At this temperature, the observed conversion during the kinetic studies was approximately 20%. Spectra collected at different time intervals during exposure of the catalyst to the full reaction mixture are shown in Fig. 13.

Bands at 1673, 1625, 1470, and 1339 cm^{-1} are formed upon the introduction of cyclohexyl chloride to the V_2O_5/TiO_2 catalyst after only 1 min on stream (Fig. 12). Identical bands were also observed at the same temperature during the adsorption of cyclohexanone onto the same catalyst, suggesting that the adsorption of cyclohexyl chloride proceeds through chlorine abstraction and the formation of a carbon–oxygen bond with the catalyst. The bands at 1673 and 1625 cm^{-1} are in the typical region for carbonyl stretching. Brabec et al. [37] have assigned higher frequency bands (i.e., 1720, 1700, and 1680 cm^{-1}) to physisorbed cyclohexanone on a HZSM-5 zeolite and a band at approximately 1650 cm^{-1} to a more strongly adsorbed cyclohexanone species held by bridging hydroxyls. Hence, the bands at 1673 and 1625 cm^{-1} in the present case can be assigned to carbonyl stretching vibrations of similar surface species exhibiting slightly different C–O bond strengths. The bands

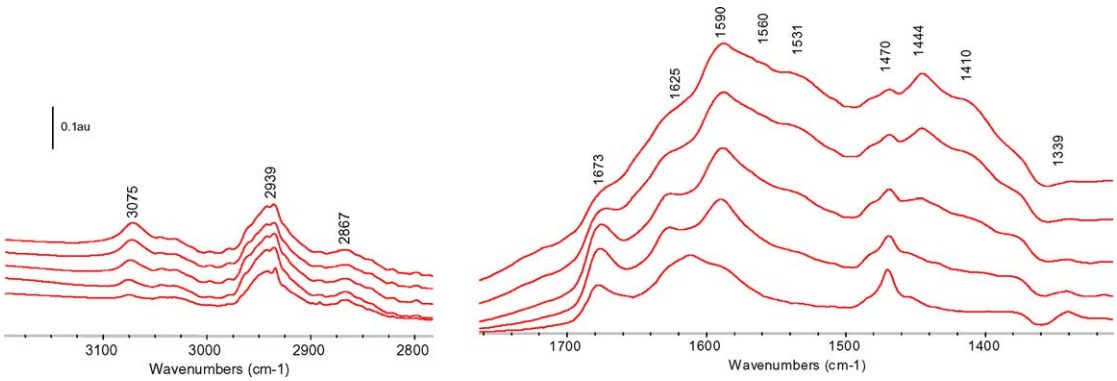

Fig. 12. In situ FTIR spectra of a 3.6 wt% V_2O_5/TiO_2 catalyst collected at 250 °C after (a) 3, (b) 10, (c) 20, (d) 40, and (e) 80 min on a 500 ppm cyclohexyl chloride/balance He stream.

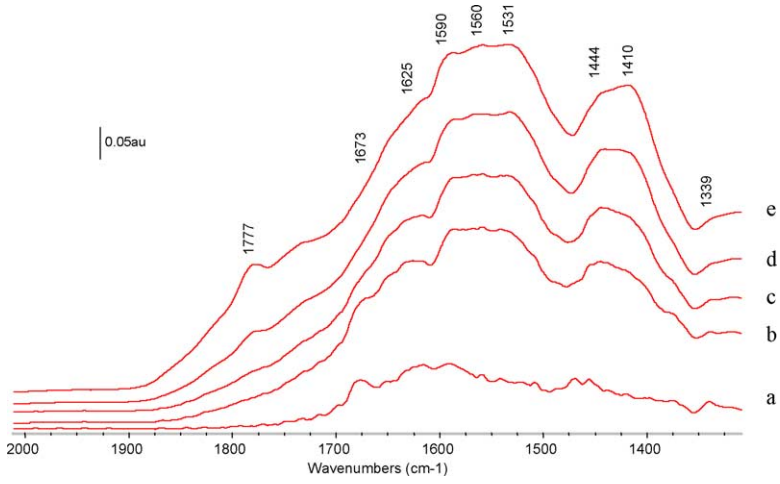

Fig. 13. In situ FTIR spectra of a 3.6 wt% V_2O_5/TiO_2 catalyst collected at 170 °C after (a) 1, (b) 5, (c) 10, (d) 20, and (e) 60 min on a 500 ppm cyclohexyl chloride/10% O_2/balance He stream.

at 1470 and 1339 cm^{-1} can be assigned to CH_2 deformation modes of an adsorbed cyclohexyl chloride [28,37,38].

A band at 1590 cm^{-1}, which grows substantially with time on stream during the adsorption of cyclohexyl chloride (Fig. 12), is also present in the spectra collected during the adsorption of cyclohexanone. Dreoni et al. [38] assigned a strong band observed at 1598 cm^{-1} during adsorption of cyclohexanone on silica at 200 °C to a C=C stretching vibration. Furthermore, these authors also assigned bands at 3075 and 3045 cm^{-1} to unsaturated =CH– bond stretchings. Indeed, a similar band at 3075 cm^{-1} was also observed in our case during the adsorption of cyclohexyl chloride and can be assigned to such a vibration mode. Additional bands in the same region at 2939 and 2867 cm^{-1} correspond to the CH stretching vibrations of the adsorbed cyclohexyl chloride [38] and are also present in the spectra of adsorbed cyclohexanone. The presence of C=C and –CH– bonds indicates the formation of the enolic form of a cyclohexanone species [38]. The intensities of the bands corresponding to this surface species decrease slightly during exposure of the catalyst to an O_2/He mixture, indicating a further reaction and/or desorption of this species.

Additional bands are present in the spectra of adsorbed cyclohexyl chloride at 1410 and 1560 cm^{-1}. The intensities of these bands increase with time on stream and remain constant during desorption. These IR peaks are in the region typical of surface carboxylates of the acetate type, as described in detail in previous paragraphs, and can be assigned to such species. Bands at 1531 and 1444 cm^{-1} can also be assigned to a surface maleate species as described in the previous section. Again, these species are stable upon desorption at 170 °C and are likely spectators on the catalyst surface. Finally, a weak band at 1777 cm^{-1}, growing in intensity during exposure of the catalyst to a O_2/He mixture, can be assigned to the O=C–O–C=O group of a cyclic anhydride [38]. An even weaker band at 1870 cm^{-1}, reportedly belonging to the same group, was not observed in our case, probably due to the small surface concentration of this species.

The same bands described above were also observed under reaction conditions (Fig. 13), suggesting once again that the oxidation process can be initiated even in the absence of gas-phase oxygen, and hence, surface oxygen is involved in the reaction. However, the relative intensities of the bands corresponding to oxygenated species, such as maleates, ac-

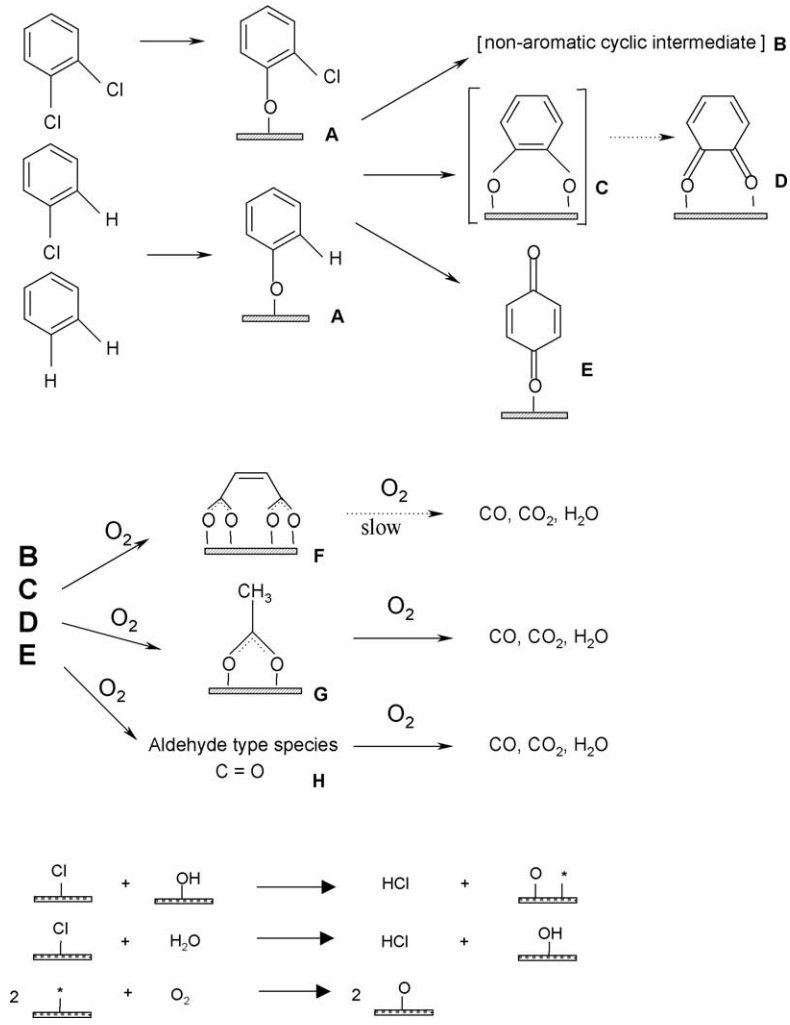

Fig. 14. Reaction mechanism for the oxidation of chlorinated benzenes over V_2O_5/TiO_2 catalysts.

etates, and anhydrides, are more pronounced in the presence of gas-phase oxygen.

3.3. Reaction mechanism

Previously, we proposed a mechanism for the oxidation of *o*-dichlorobenzene over supported vanadia catalysts [39]. The additional kinetic and FTIR results obtained in the current study suggest that the oxidation of different chlorinated benzenes takes place over V_2O_5/TiO_2 via a similar pathway. Furthermore, the similarities and differences observed with the different compounds studied can be used to obtain estimates for the relative rates of the individual steps involved in the proposed mechanism.

Based on the results obtained in the current as well as our previous kinetic and spectroscopic studies, we propose that the oxidation of chlorinated benzenes over V_2O_5/TiO_2 catalysts proceeds through the mechanism shown in Fig. 14. The first step of this mechanism is believed to be a nucleophilic substitution. Surface phenolates (A) are formed during this step as indicated by the in situ FTIR results. The reactivity of aryl halides toward nucleophiles is enhanced in the presence of electron-withdrawing substituents (i.e., C–Cl bonds are weaker than C–H bonds, and hence, more prone to attack by nucleophiles). Consequently, the first step in the oxidation of chlorinated benzenes is their dissociative adsorption on a transition metal oxide site via Cl abstraction. Dichlorobenzenes offer two positions for such a nucleophilic attack, while only one such position exists in chlorobenzene. This difference can explain the slightly higher activation energy observed with the latter. Furthermore, the nucleophilic attack on the nonchlorinated benzene molecule is substantially more difficult in the absence of any electron-withdrawing groups, resulting in a significantly higher activation energy. Further support for the nucleophilic nature of the adsorption step can be found in the results obtained with the pure titania support, in which case the adsorption of *m*-DCB leads to the formation of a surface phenolate, while no such species is formed during benzene adsorption. The involvement of nucleophilic oxygen species (i.e., O^{2-} ions on oxidized cationic sites) in the mechanisms of both the selective and the complete oxidation of hydro-

carbons over $MgCr_2O_4$ has also been proposed by Finocchio et al. [40]. The proposed nucleophilic attack is also consistent with the conclusions of van den Brink et al. [41] who reported that C–Cl bond scission is the first step of the oxidation of chlorobenzene over Pt/γ-Al_2O_3 and takes place even at room temperature. These authors also reported a substantial kinetic isotope effect for the oxidation of deuterated benzene, while only a small difference was observed in the case of perdeuterochlorobenzene, supporting the notion that the latter is activated by the weaker C–Cl and not the C–H bond.

The second step of the proposed mechanism is an electrophilic substitution of the adsorbed partially dechlorinated species. Benzene and chlorobenzene form the same adsorbed species, since chlorobenzene is fully dechlorinated during the adsorption process. The proposed electrophilic attack on this species is expected to be faster than the corresponding attack on the adsorbed dichlorobenzene derivatives, which still have one chlorine atom attached to their ring structures, since halogen substituents are deactivating toward electrophilic substitution reactions. The proposed electrophilic substitution is further supported by the differences observed in the kinetic results obtained with the different dichlorobenzene isomers. In particular, chlorine is known to be an *ortho-para* director during electrophilic substitutions. During the nucleophilic substitution of the first step one of the chlorine atoms is abstracted and replaced by a surface oxygen species. The *ortho-para*-directing effect of the Cl substituent is then enhanced by the surface oxygen, which is also known to be *ortho-para* directing. However, considering the structures of the different adsorbed dichlorobenzene isomers, the *m*-DCB surface derivative is the only one exhibiting two positions that are *ortho* to one of the substituents and *para* to the other. Hence, the surface species derived from *m*-DCB is expected to undergo an electrophilc attack more easily than the surface species derived from the other two dichlorobenzene isomers. The spectroscopic results obtained suggest that surface phenolates exist in higher concentrations during adsorption/reaction of *m*-DCB as compared to benzene, suggesting that phenolates are formed easier in the case of dichlorobenzene and/or undergo reaction faster in the case of benzene. These observations are consistent with the proposed reaction mechanism, and the nucleophilic and electrohilic nature, respectively, of the first two steps. Hence, we anticipate a faster initial and a slower second step for *m*-DCB as compared to the benzene.

As observed spectroscopically the second step of the proposed reaction mechanism can lead to the formation of *o*-benzoquinone (D) (formed through a surface catecholate (C)) or *p*-benzoquinone (E). These species can react further in a subsequent step to form the surface maleates (F) and acetates (G) observed spectroscopically. The electrophilic substitution could also result in the bond breaking of the aromatic ring to give a nonaromatic intermediate (B), which reacts rapidly to form surface maleates (F), acetates (G), and aldehydes (H). The destruction of the aromatic ring during the electrophilic attack is more probable in the case of dichlorobenzene. This hypothesis is supported by the presence of *o*-benzoquinone on the catalyst surface during the reaction/adsorption of benzene, which was not observed during the corresponding reaction/adsorption of *m*-DCB. The proposed electrophilic attack in this case takes place on a hydrogen atom, and hence, both the electrophilic substitution and the abstraction of the second chlorine may occur simultaneously and interrupt the aromaticity.

Some of the partial oxidation products formed on the surface can undergo further reaction to form the gas-phase reaction products, observed during the kinetic studies (i.e., CO, CO_2, HCl, and H_2O). Surface maleates are fairly stable on the catalyst surface as indicated by the FTIR results and may represent spectator species at least in the lower temperature regime. Since surface maleates and acetates are observed on the V_2O_5/TiO_2 catalyst surface during adsorption/reaction of the aromatic compounds even in the absence of gas-phase oxygen, it is clear that surface oxygen is involved in their formation. As expected, gas-phase oxygen, when present, replenishes the catalyst surface, hence enhancing the rate of formation of surface partial oxidation products. The catalyst surface is dechlorinated through reaction with surface hydroxyl groups and/or water. Finally, the catalyst surface is reoxidized by gas-phase oxygen in a fast step, as indicated by the observed zero-order kinetics in oxygen under the excess oxygen conditions used [16].

4. Conclusion

The oxidation of different chlorinated benzenes (i.e., chlorobenzene, 1,2- 1,3-, and 1,4-dichlorobenzene), as well as the oxidation of benzene and cyclohexyl chloride, was investigated over a 3.6 wt% V_2O_5/TiO_2 catalyst. The kinetic results revealed that (i) cyclohexyl chloride was easier to oxidize than any of the aromatic compounds, indicating that the destruction of the aromatic ring is a slow and kinetically significant step, (ii) the activation of the chlorinated aromatic compounds was easier than the activation of benzene, suggesting that electron-withdrawing groups enhance this process, and (iii) the degree of chlorination and relative position of the chlorine atoms on the aromatic ring affect the oxidation behavior.

In situ FTIR experiments revealed that similar surface species (i.e., phenolates, quinones, acetates, and maleates) are formed on the V_2O_5/TiO_2 surface during the reaction of both benzene and *m*-DCB. Combined, the kinetic and spectroscopic results suggest that a common reaction mechanism is operating during the oxidation of all compounds studied. The main steps of this reaction pathway are the adsorption of the aromatic compound via a nucleophilic substitution and its further reaction via an electrophilic substitution. Partial oxidation products are formed in both the presence and the absence of gas-phase oxygen, indicating that surface oxygen is involved in the oxidation process.

References

[1] R. Weber, T. Sakurai, H. Hagenmeier, Appl. Catal. B 20 (1999) 249.
[2] K.B. Carlsson, Chemosphere 25 (1992) 135.
[3] R. Boos, R. Budin, H. Hartl, M. Stock, F. Wurst, Chemosphere 25 (1992) 375.
[4] R. Weber, T. Sakurai, Appl. Catal. B 34 (2001) 113.
[5] G. Busca, M. Baldi, C. Pistarino, J.M. Gallardo Amores, V. Sanchez Escribano, E. Finocchio, G. Romezzano, F. Bregani, G.P. Toledo, Catal. Today 53 (1999) 525.
[6] M. Stoll, J. Furrer, H. Seifert, G. Schaub, D. Unruh, Waste Manage. 21 (2001) 457.
[7] T. Sakurai, R. Weber, Organohalogen Compounds 36 (1998) 275.
[8] J. Jones, J.R.H. Ross, Catal. Today 35 (1997) 97.
[9] R.M. Lago, M.L.H. Green, S.C. Tsang, M. Odlyha, Appl. Catal. B 8 (1996) 107.
[10] S. Krishnamoorthy, J.P. Baker, M.D. Amiridis, Catal. Today 40 (1998) 39.
[11] R.W. van den Brink, R. Louw, P. Mulder, Appl. Catal. B 16 (1998) 219.
[12] I.M. Freidel, A.C. Frost, K.J. Herbert, F.J. Meyer, J.C. Summers, Catal. Today 17 (1993) 367.
[13] G.R. Lester, R.F. Renneke, K.J. Herbert, in: Proceeding of the 1992 Air & Waste Management Assoc. Annual Meeting, Kansas City, MO, 1992.
[14] G. Sinquin, J.P. Hindermann, C. Petit, A. Kiennemann, Catal. Today 54 (1999) 107.
[15] Y. Liu, M. Luo, Z. Wei, Q. Xin, P. Ying, C. Li, Appl. Catal. B 29 (2001) 61.
[16] S. Krishnamoorthy, M.D. Amiridis, Catal. Today 51 (2) (1999) 3.
[17] S. Krishnamoorthy, J.A. Rivas, M.D. Amiridis, J. Catal. 193 (2000) 264.
[18] J. Furrer, M. Stoll, R. Bechtler, H. Seifert, G. Schaub, in: Proceedings of the 1999 International Conference on Incineration, 1999, p. 327.
[19] G. Busca, G. Ramis, V. Lorenzelli, in: G. Centi, F. Trifiro (Eds.), New Developments in Selective Oxidation, Elsevier, Amsterdam, 1990.
[20] H. Miyata, T. Ohno, F. Hitayama, J. Chem. Soc., Faraday Trans. 91 (1995) 3505.
[21] L. Palmisano, M. Schiavello, A. Sclafani, G. Martra, E. Borello, S. Coluccia, Appl. Catal. B 3 (1994) 117.
[22] J. Bandara, J.A. Mielczarski, J. Kiwi, Appl. Catal. B 34 (2001) 307.
[23] A.J. van Hengstum, J. Pranger, S.M. van Hengstum-Nijhuis, J.G. van Ommen, P.J. Gellings, J. Catal. 101 (1986) 323.
[24] S.C. Street, Q. Guo, C. Xu, D.W. Goodman, J. Phys. Chem. 100 (1996) 17599.
[25] F. Hatayama, T. Ohno, T. Maruoka, H. Miyata, React. Kinet. Catal. Lett. 45 (1991) 265.
[26] R. Ramstetter, M. Baerns, J. Catal. 109 (1988) 303.
[27] G. Busca, G. Ramis, V. Lorenzelli, J. Mol. Catal. 55 (1989) 11.
[28] D. Lin-Vien, N.B. Colthup, W.G. Fateley, J.G. Grasselli, The Handbook of Infrared and Raman Characteristic Frequencies of Organic Molecules, Academic Press, San Diego, 1991.
[29] V.E. Suprunov, A.A. Ivanov, React. Kinet. Catal. Lett. 33 (1987) 75.
[30] P.S. Chintwar, H.L. Greene, J. Catal. 165 (1997) 12.
[31] V.S. Escribano, G. Busca, V. Lorenzelli, J. Phys. Chem. 94 (1990) 8939.
[32] E. Finocchio, G. Busca, V. Lorenzelli, R. Willey, J. Chem. Soc., Faraday Trans. 90 (1994) 3347.
[33] E. Spinner, J. Chem. Soc. (1964) 4217.
[34] L.M. Ng, E. Lyth, M.V. Zeller, D.L. Boyd, Langmuir 11 (1995) 127.
[35] W. Otting, G. Staiger, Chem. Ber. 88 (1955) 802.
[36] S. Lomnicki, J. Lichtenberger, Z. Xu, M. Waters, J. Kosman, M.D. Amiridis, Appl. Catal. B, in press.
[37] L. Brabec, J. Novakova, L. Kubelkova, J. Mol. Catal. 94 (1994) 243.
[38] D.P. Dreoni, D. Pinelli, F. Trifiro, G. Busca, V. Lorenzelli, J. Mol. Catal. 71 (1992) 111.
[39] S. Krishnamoorthy, PhD thesis, University of South Carolina, 1999.
[40] E. Finocchia, G. Busca, V. Lorenzelli, R.J. Willey, J. Catal. 151 (1995) 204.
[41] R.W. van den Brink, V. de Jong, R. Louw, P. Maggi, P. Mulder, Catal. Lett. 71 (2001) 15.